Chemical Engineering Journal 219 (2013) 254–261

Contents lists available at SciVerse ScienceDirect

Chemical Engineering Journal

journal homepage: www.elsevier.com/locate/cej

Ultrasound assisted synthesis and characterization of poly(methyl methacrylate)/$CaCO_3$ nanocomposites

Krishnamurthy Prasad [a], Shirish Sonawane [b], Meifang Zhou [a], Muthupandian Ashokkumar [a,*]

[a] School of Chemistry, University of Melbourne, Parkville, VIC 3010, Australia
[b] Chemical Engineering Department, National Institute of Technology, Warangal, AP 506 007, India

HIGHLIGHTS

- Combined use of ultrasound and conventional chemical initiation improves final conversion.
- Combined technique offers smaller particle size and narrow size distribution.
- Composite and core–shell particles obtained explained by dual pathway mechanism.

ARTICLE INFO

Article history:
Received 3 September 2012
Received in revised form 31 October 2012
Accepted 5 January 2013
Available online 11 January 2013

Keywords:
Ultrasound
PMMA
$CaCO_3$
Nanocomposites
Emulsion polymerization

ABSTRACT

The combined effects of sonochemical and conventional chemical initiation on the emulsion polymerization of methyl methacrylate (MMA) and MMA–$CaCO_3$ systems have been studied. Combining ultrasound (US) and conventional initiation by potassium persulfate (KPS) for the MMA and MMA–$CaCO_3$ systems, helped increase the final conversion. An increase of 15% for the MMA only system (from 72% to 87%) and of 10% for the MMA–$CaCO_3$ system (from 76% to 86%) was observed as compared to initiation by KPS alone. Also, an increase of 18% (from 69% to 87%) and 20% (from 66% to 86%) for the MMA only and MMA–$CaCO_3$ systems, respectively was observed for the combined initiation as compared to initiation by US alone. Although all particles synthesized were in the size range of 60–130 nm, the excellent dispersion ability of ultrasound helped to obtain narrow size distribution and smaller average sizes in both the PMMA and PMMA–$CaCO_3$ systems. Possible mechanisms have been proposed for both the polymerization and the formation of poly-MMA–$CaCO_3$ composite and core–shell nanoparticles taking into account the results obtained by analyzing the synthesized materials.

1. Introduction

The chemical effects of ultrasound have been well-explained as the consequence of localized hot spots created during the collapse of cavitation bubble. The collapse of bubbles produces intense local heating (~5000 K) and high pressures (~1000 atm) with very short lifetimes and heating and cooling rates above 10^{10} K/s [1]. The different ways in which ultrasonic input can beneficially affect a chemical reaction have been discussed [2] and such beneficial effects have been used for (amongst other things) carrying out emulsion polymerization [3] of monomers like methyl methacrylate [4,5], butyl acrylate [6,7] and styrene [8–10].

The results from these studies have proven the efficacy of the use of ultrasound in emulsion polymerization. First, the physical effects, generated by the cavitation process, act to disperse approximately uniformly sized monomer droplets in the aqueous phase. The (primary) H and OH radicals created by the sonolytic decomposition of water react with the monomer generating monomeric radicals. Also, the monomer itself can evaporate into the cavitation bubbles and decompose (on bubble collapse) to create secondary radicals which will also help create more monomeric and other radicals. These radicals then diffuse into the surfactant stabilized monomer droplets and initiate the polymerization reaction converting the droplet into a polymer latex particle. Ultrasound assisted emulsion polymerization has several advantages over the conventional emulsion polymerization [4].

There has also been a large body of work on synthesizing composite emulsions, i.e., those consisting of a polymer in combination with an inorganic phase using ultrasound assisted emulsion polymerization [11–16]. An extensive review on this topic has been reported by Gedanken [17]. The reasons for encapsulating an inorganic material in a polymeric matrix include improving the abrasion resistance of the parent polymer [18], improving the thermal resistance [19], imparting anticorrosive properties [11], etc. The addition of inorganic particles during emulsion polymerization

* Corresponding author. Tel.: +61 3 83447090; fax: +61 3 93475180.
E-mail address: masho@unimelb.edu.au (M. Ashokkumar).

1385-8947/$ - see front matter © 2013 Elsevier B.V. All rights reserved.
http://dx.doi.org/10.1016/j.cej.2013.01.012

may destabilise the system (depending upon the nature of the inorganic particles) that may lead to agglomeration of the particles. Hence, a specialized process is needed in the case of encapsulation in order to create homogeneous dispersion of inorganic particles in the polymer matrix [11]. It has been found that ultrasound input can provide enough energy to effectively disperse such inorganic particles and can intensify the reaction with increase in conversions. In addition, there can be (in some cases) a reduction in overall energy requirements [12]. The effective dispersion also helps exert control on the particle size distribution and this is an important characteristic of the ultrasound-assisted emulsion polymerization technique.

Initiating polymerization in an MMA emulsion system to synthesize PMMA using chemical initiation by thermal energy (after which will be referred to as conventional initiation) has been extensively studied [20–22] and similarly a large body of work has been reported on the ultrasound-initiated emulsion polymerization of MMA [23–25]. The mechanisms of ultrasound-initiated emulsion polymerization [25] and of conventional emulsion polymerization [26] are well understood. It has been generally observed that ultrasonic polymerization is a relatively slow process with the generation of relatively smaller size and narrow size distribution of particles. The extent of radical formation by ultrasound is generally lower than what is observed for conventional chemical initiation (decomposition of KPS to yield SO_4 radicals) and thus the rates for the US reactions are lower than those for the NUS. Whilst the conventional polymerization process is faster with the generation of relatively larger size and broader size distribution of particles. A combination of the conventional and ultrasound-assisted polymerization may have advantages of both methods in terms of optimized conversion rate along with controlled particle size and size distribution. While the combination of ultrasound and conventional processes has been reported [27,28], a detailed mechanism on the combined effects of ultrasound and conventional processes is still lacking. In this study, we have attempted the emulsion polymerization based synthesis of PMMA and PMMA-$CaCO_3$ nanocomposite systems using a combined method involving conventional and ultrasonic polymerization. In order to compare the results, polymer nanocomposites have also been prepared using individual techniques, despite reported in earlier studies [11–16].

2. Experimental

2.1. Materials

Methyl methacrylate (MMA, density: 0.936 g/cm^3 AR grade) was procured from Sigma Aldrich and was used after the removal of inhibitors by filtering twice through powdered alumina. The surfactant, sodium dodecylsulfate (SDS, AR grade) was obtained from BDH Ltd., and the initiator potassium persulfate (KPS, $K_2S_2O_8$, AR grade) was procured from Ajax Finechem Ltd., and both were used without further purification. Myristic acid (MA) coated $CaCO_3$ used in this study was synthesized by a procedure reported by Bhanvase et al. [12].

2.2. Apparatus

All reactions were carried out in a custom made glass cell fitted with a water jacket through which thermostated water was circulated to maintain the required temperature. The ultrasound equipment employed for the sonochemical polymerization reactions was a Branson 450, 20 kHz ultrasound generator, with a standard horn of 19 mm in diameter with a stainless steel tip. All reactions were carried out in millipore water. High purity argon was used to maintain an inert atmosphere for the duration of the reaction.

2.3. Synthesis of polymer nanocomposites

2.3.1. MMA only polymerization

The process involved making a solution of SDS in water and then, MMA and (if required) KPS were added to the solution. The mixture was then purged with argon gas for 45 min to deaerate the solution. After sparging the emulsion, the bubbling of argon through the reaction mixture was stopped and the gas was allowed to pass over the reaction mixture. At this time, the water in the jacket of the reactor was set at the required temperature. The reaction was then carried out for 1 h at the desired temperature. On the basis of the use of initiator (or lack of) there were three separate reaction systems, viz.,

- Non-Ultrasound (NUS) process: only KPS was used to initiate polymerization. The NUS process was provided with mechanical stirring by means of a Steristirrer (Sterimed Ltd. Melb.) magnetic stirrer.
- Ultrasound (US) process: only ultrasound was used to initiate polymerization. The US was delivered at a pulsed input (0.7 s on, 0.3 s off) with 50% amplitude corresponding to a calorimetrically determined effective power delivery of 23 W. Before argon purging, the liquid mixture was sonicated for 20 s in continuous mode (corresponding to a calorimetrically determined effective power delivery of 29 W). Due to the initial continuous mode pulse, the MMA was dispersed as fine droplets that were stabilized by SDS, which prevented the volatilization.
- USK or Ultrasound KPS: a combination of ultrasound and KPS was used to initiate polymerization. The ultrasonic experimental conditions used were similar to that used for US only system.

The amounts of MMA, SDS and water were used as in Teo et al. [4], specifically, 7.5 g MMA, 0.55 g SDS and 69 g water. All reactions were carried out from 20 °C to 50 °C. All NUS and USK reactions were carried out in the presence of 0.3 g of KPS. The US only reactions did not use any KPS. The reactions were referred to with the type of reaction (NUS, US or USK) followed by the temperature (20, 30, 40 or 50 °C) for instance a NUS MMA only reaction carried out at 20 °C was referred to as NUS 20, a USK MMA only reaction carried out at 30 °C was referred to as USK 30, etc.

2.3.2. MMA–$CaCO_3$ nanocomposite

The process for synthesizing the poly-MMA–$CaCO_3$ nanocomposites was similar to the MMA only reactions, the only difference being that the myristic acid coated $CaCO_3$ was added to the solution of SDS in water and a uniform suspension of $CaCO_3$ was formed. Similar to the MMA only reactions, there were three sets of reactions, the details of which have already explained in Section 2.3.1. There was a slight difference in notation while referring to the reactions. The use of 4 wt.% $CaCO_3$ (with respect to MMA) corresponding to 0.3 g of $CaCO_3$ necessitated the inclusion of 'C' in the reactions names. For instance, a NUS MMA–$CaCO_3$ reaction carried out at 20 °C was referred to as NUSC 20, a USK MMA–$CaCO_3$ reactions carried out at 30 °C was referred to as USKC 30, etc.

2.4. Percentage conversion

The percentage of monomer conversion to polymer was determined by using gravimetric analysis. During sonication, aliquots of the reaction mixture were removed every 10 min of reaction time. These samples were dried in an oven overnight at ~100 °C to remove water and unreacted monomer leaving behind a residue containing the polymer, initiator (if any) and surfactant (in case of

the MMA–$CACO_3$ system, an additional material was $CaCO_3$). As the amount of the surfactant and initiator were known, the overall conversion of monomer to polymer could be estimated.

2.5. Particle size measurement

The sonicated samples were diluted by a factor of ~100 in millipore water and particle size measurements were performed using a dynamic light scattering instrument (Malvern Zetasizer).

2.6. X-ray diffraction (XRD)

A part of the synthesized emulsions were precipitated with methanol and dried in an oven at ~100 °C overnight. The dried samples were then analyzed by XRD using a Bruker D-8 Advance in a 2θ range of 5–80°.

2.7. Scanning electron microscopy (SEM) and transmission electron microscopy (TEM)

The precipitated samples were also analyzed for their morphological properties using SEM and TEM. The SEM was carried out on a FEI Quanta operated at an acceleration voltage of 10 kV and the TEM was carried out on a FEI TF20 Tecnai G2 machine operated at 200 kV.

3. Results and discussions

The main purpose of this investigation was to study the combined effects of ultrasound and conventional initiation by KPS on an emulsion polymerization process. A possible mechanism of polymerization and particle formation has been suggested, taking into account the interaction between the sonochemically and conventionally generated radicals.

3.1. Conversion and kinetics of MMA only reactions

The mechanism of a chemical initiator aided emulsion polymerization first involves the reaction of the monomer present in the aqueous phase with the initiator radicals forming a monomer radical that later grows in size by reacting with other monomer molecules forming oligomeric radicals [26]. These oligomeric radicals thus increase in hydrophobicity and after reaching a certain chain length, diffuse into the stabilized monomer droplets initiating polymerization. Thereafter, these droplets are successfully transformed into polymer particles [26].

Table 1
First order rate constants for all the polymerization reactions studied.

Reaction	Rate constant (s^{-1})			
	20 °C	30 °C	40 °C	50 °C
NUS	0.24	0.43	1.05	1.66
US	0.85	1.20	1.00	0.86
USK	0.65	0.86	1.04	1.72
NUSC	0.47	0.64	1.41	1.84
USC	0.58	1.29	0.82	0.59
USKC	0.32	0.46	1.47	2.03
NUSC 0.1[a]	–	–	–	1.82
USC 0.1 [a]	–	1.15	–	–
USKC 0.1 [a]	–	–	–	1.96

[a] 0.1 Refers to the amount of $CaCO_3$ added which is 0.1 g.

For all the reactions, the variation of % conversion with time was estimated and the data was analyzed using first order kinetics. In studies conducted by Prescott et al. [29] and Teo et al. [4], the reasons for why emulsion polymerization may follow a zero-one model were discussed. The basis of the zero-one model suggests that the rate of polymerization shows a first order dependency with the monomer concentration.

3.1.1. KPS initiated NUS polymerization of MMA

As seen from Fig. 1a, there is an increase in final conversion (from 18% at 20 °C to 78% at 50 °C) with an increase in solution temperature. At low temperatures (20 °C and 30 °C), initial conversions are lower (9.3% and 13.5%, respectively at 20 min reaction time) and there is a gradual increase in conversion with time. At higher temperatures (40 °C and 50 °C), initial conversions are higher (42.9% and 66.7%, respectively at 20 min reaction time) and maximum conversion is reached faster (especially at 50 °C, where the conversion is almost constant from 30 min of reaction time onwards). All reactions seem to follow first order kinetics (Fig. 1b).

Similar data was obtained for all remaining reactions (and all of them followed first order kinetics) but the results shown from now on are the rate constants obtained from the kinetic fits. The values are tabulated in Table 1. It can be seen that the rate constants for the NUS reactions increased with increase in temperature and the rate constant at 50 °C (2.54 s^{-1}) is about ten times higher than that observed at 20 °C (0.24 s^{-1}).

KPS is thermally decomposed to generate $SO_4^{\cdot-}$ radicals that initiate the polymerization process. The rate of decomposition of KPS

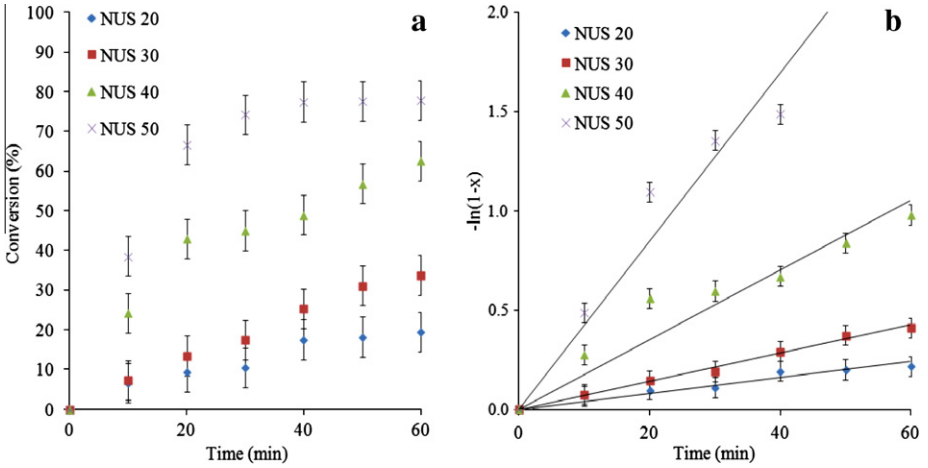

Fig. 1. (a) Monomer conversion as a function of time for MMA only NUS reactions. (b) First order kinetic treatment (x as the fractional conversion of the monomer) as a function of sonication time for MMA only NUS reactions.

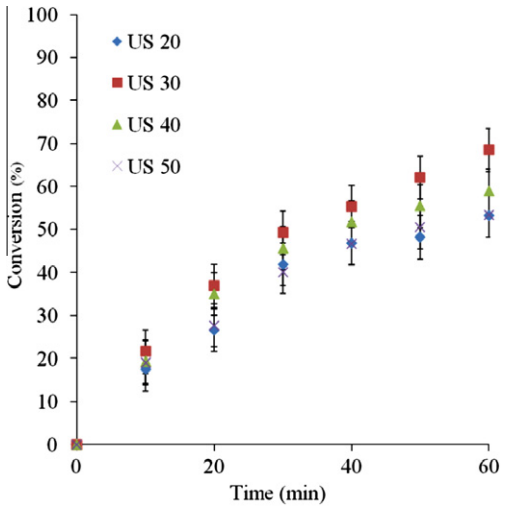

Fig. 2. Monomer conversion as a function of time for MMA only US reactions.

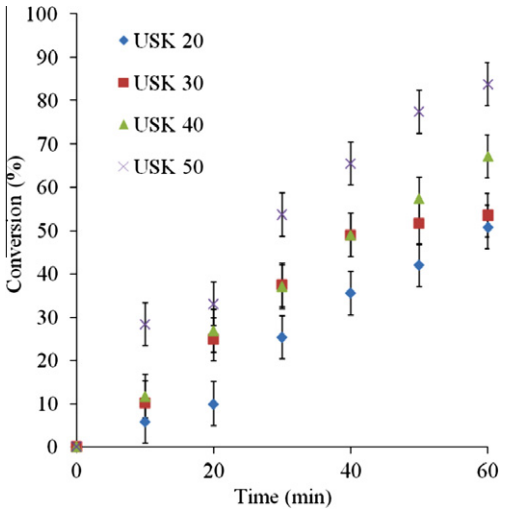

Fig. 3. Monomer conversion as a function of time for MMA only USK reactions.

is temperature dependent and increases with an increase in temperature [30]. In addition, the propagation reaction rate constant may be higher at higher temperatures as per the Arrhenius equation. Due to the above mentioned reasons, the rate of polymerization is higher at higher temperatures. The NUS reactions showed a high initial rate of conversion on account of the large number of radicals produced and the consequent higher rates of reaction. The rate of polymerization is directly proportional to the monomer concentration and such a rapid consumption of monomer leading to a significant lowering of monomer concentration, leads to a large reduction in polymerization rates with time. Also, at high conversions the process of monomer transport to the polymerization loci (vicinity of growing polymeric radicals) via diffusion becomes the rate controlling step [31] resulting in a lowering of polymerization rate. Thus, the rate of polymerization is greatly diminished and hence, the conversions achieve near constant value. Theoretically, emulsion polymerization processes are supposed to go to 100% conversion. However, at higher temperatures, the volatility of the monomer MMA becomes a factor [4]. Due to a marked increase in its vapor pressure, a significant part of the monomer evaporates. In addition, as the water solubility of MMA is higher at higher temperatures, the probability of MMA dissolving in the aqueous phase and participating in side reactions is very high. Both these factors contribute in the non-achievement of 100% conversion.

3.1.2. US initiated polymerization of MMA

The % conversion for US initiated polymerization of MMA is shown in Fig. 2. Note that the ultrasonic polymerization of MMA has been previously reported [4,5]. The reason for repeating this work was for comparison purposes under the experimental conditions used in this study. The highest conversion amongst the various reactions carried out solely using US was obtained at 30 °C (68.5%). There is an increase in final conversion from 20 °C (53.2%) to 30 °C (68.5%), after which there is a reduction at 50 °C (53.3%), showing the least conversion (unlike the NUS system where 50 °C showed the maximum conversion). With all the reactions, there is a gradual increase in conversion with time, with the reactions gradually slowing down as time proceeds. The rate constants (Table 1) for the reactions initially increase (from 0.85 s^{-1} at 20 °C to 1.20 s^{-1} at 30 °C) and then decrease (0.86 s^{-1} at 50 °C), suggesting that lower temperatures are more suited for ultrasound assisted polymerization as was also shown by Price [3].

The mechanistic pathway for the US reactions involves first, the sonolysis of water creating H and OH radicals [25]. Some researchers have also suggested that the source of radicals may also be obtained by the degradation of the surfactant molecules [24]. In addition, the volatile monomer may evaporate into the bubble and generate other radicals within the bubbles. Thus, a variety of radicals are generated by ultrasound input, viz., H and OH radicals by sonolysis of water and the alkyl radicals from the surfactant and monomer. These radicals attack the monomer molecules, leading to the creation of monomer radicals. These monomer radicals then enter the surfactant stabilized monomer droplets and initiate the polymerization process. The major difference between the conversion patterns of the US reactions and the NUS reactions is that the increase in conversion with time for the US reactions occurs gradually. In case of the NUS process, the amount of radicals generated is much higher than the radials generated by the US process in the same time period. After 1 h of sonication at 20 kHz around 10 μM of OH radicals could be generated [1] while starting with a 0.01 M concentration of KPS could result in as much as 35 μM of $SO_4^{\cdot-}$ radicals in the same time period [32]. Therefore, the rate of radical production with time, in case of the US process is more gradual as compared to the NUS process, leading to the increase in conversions for the US process to be gradual as well.

3.1.3. Ultrasound with KPS (USK) initiated polymerization of MMA

In the case of the USK reactions, high conversions are obtained accompanied by an increase in conversion with temperature (Fig. 3). Unlike the NUS reactions, at higher temperature the conversions gradually increase with time (50.8% at 20 °C to 83.8% at 50 °C). Like the NUS system, high conversions are observed indicating that the reaction may proceed to completion. USK reactions show an increase in overall conversion compared to NUS and US only reactions, but the rate of conversion is relatively slow compared to the NUS reactions. Mirroring the trends in conversion, the rate constants for the reactions also increase with temperature with the rate constant at 50 °C (1.72 s^{-1}) being around three times higher than that at 20 °C (0.65 s^{-1}).

The USK reactions combine the advantages of NUS and US only reactions. The USK system can be expected to produce three sets of radicals, viz.; the $SO_4^{\cdot-}$ radicals generated thermally, the H and OH radicals by the sonolysis of water and the radicals created by the sonochemical degradation of the surfactant and monomer molecules. Thus, theoretically, generation of more radicals in the USK system compared to the individual systems should ensure a very large number of initiation reactions and consequently, the initial rates of polymerization should be very high leading to high initial

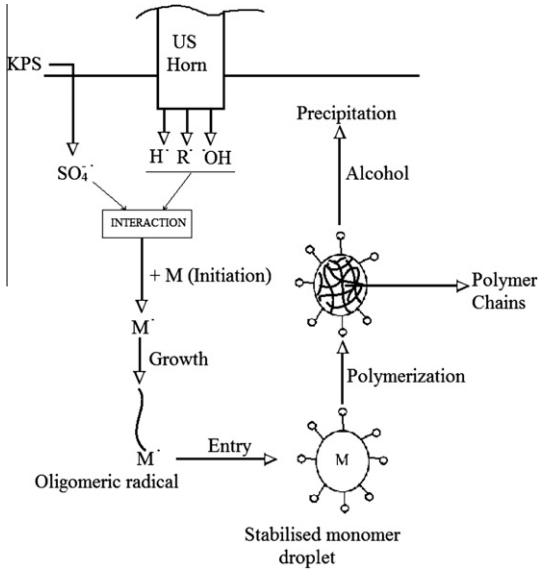

Fig. 4. Mechanism of USK polymerization and particle formation.

conversions. However, rate of conversion is relatively slow compared to NUS only, which might be due to other interfering reactions. The highly reactive $SO_4^{\cdot-}$ radical anion may react with H, OH, surfactant and monomer radicals generated by sonication and hence, the total amount of radicals available for initiation is reduced. The three possible reactions for the $SO_4^{\cdot-}$ radical are as follows [33–35]:

$$SO_4^{\cdot-} + M \xrightarrow{k_1} M^{\cdot} + SO_4^{2-} \quad k_1 = 1 \times 10^9\ M^{-1}\ s^{-1} \tag{1}$$

$$OH^{\cdot} + M \xrightarrow{k_2} M^{\cdot} + OH^{-} \quad k_2 = 1.19 \times 10^{10}\ M^{-1}\ s^{-1} \tag{2}$$

$$SO_4^{\cdot-} + OH^{\cdot} \xrightarrow{k_3} HSO_4^{-} + 1/2O_2 \quad k_3 = 1 \times 10^9 - 1 \times 10^{10}\ M^{-1}\ s^{-1} \tag{3}$$

It can be seen that the rate constants k_2 and k_3 are almost equal (considering the higher value for k_3) and both are higher than k_1. It can be suggested that the sulfate radical is consumed in Reaction 3, thus reducing its availability for Reaction 1. Therefore, the mechanism proposed for USK reactions involves regulation of sulfate radical concentration by reaction with other radical species leading to lower initial rates. However, the radical production at 50 °C is high enough in total to lead to a higher final conversion over the same period of time as compared to both the NUS and US only reactions.

Thus, the USK reaction provides positive results by increasing final conversion but acted detrimentally in slowing down the initial reaction rates. However, this drawback is over compensated by the reduced size and narrow size distribution of the polymer particles generated compared to the NUS system (further discussion on this aspect is provided later). On the basis of the results a mechanism for the USK reaction is proposed as below (Fig. 4).

The mechanism included firstly, the formation of three sets of radicals, their subsequent interaction, reaction and neutralization. The remaining 'useful' radicals then participate in initiation, after which the polymerization proceeds as described by Chern [26].

In addition to increasing the final conversion, USK system has also shown a significant effect on the particle size and size distribution compared to the NUS system. The NUS system had a predominantly wide size distribution as compared to the US and USK systems (Fig. 5a). In addition, the NUS system also had a higher average particle size as compared to the other two systems. From the size distribution it is also visible that there are relatively a higher number of larger particles in the NUS system compared to the US and USK systems (Fig. 5a). The SEM of the precipitated USK 50 (Fig. 5b) shows that the material consisted of small spherical particles, consistent with the particle size distribution data.

Acoustic cavitation generates shear forces that disperse monomer droplets in solution and reducing them to a very small size. Each individual droplet is polymerized creating small sized stabilized polymeric particles [25]. Thus, small sized and narrow size distribution particles were generated in case of the US and USK systems. The absence of such shear forces in the NUS systems results in the generation of relatively larger droplets and hence resulted in a product with a wider particle size distribution.

Overall, the US alone reaction is slow, offers lower final conversions but with a smaller particle size and narrow particle size distribution. The NUS reactions offer faster reaction with high conversions but with a wide particle size distribution and larger average size. By an effective combination of the two processes, a relatively higher rate of reaction (as compared to US) is obtained with a narrow particle size distribution and lower average particle size (as compared to the NUS reactions).

3.2. MMA–$CaCO_3$ system

After studying the MMA only reactions, an attempt was made to study the polymerization of MMA but with incorporation of myris-

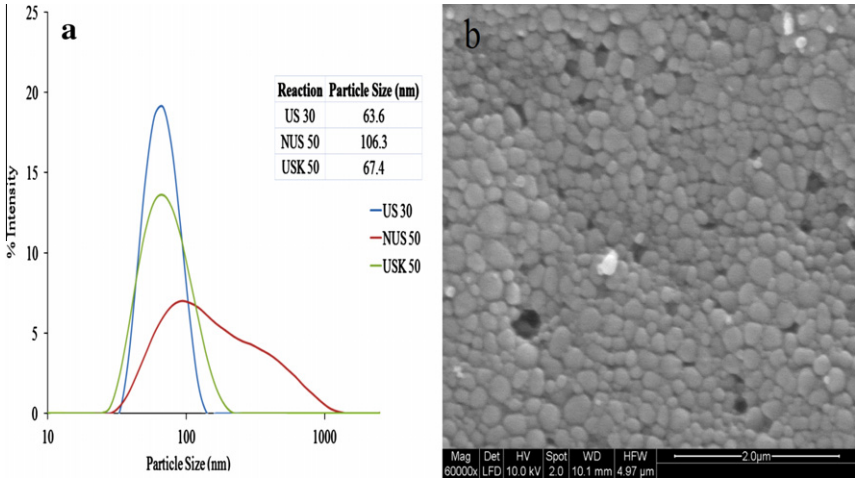

Fig. 5. (a) Particle size distributions of the polymer particles generated by US, NUS and USK methods. (b) SEM micrograph of the polymer particles generated by USK 50.

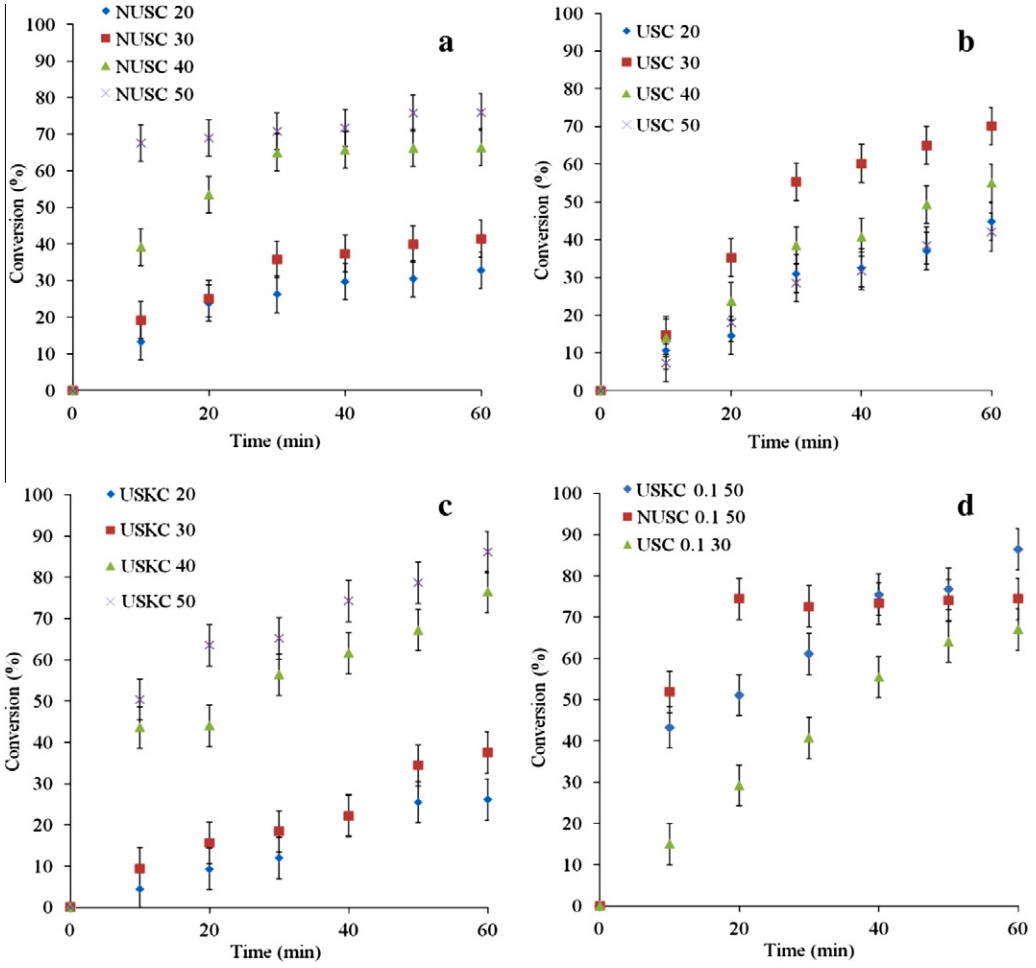

Fig. 6. Conversion % as a function of time for MMA–$CaCO_3$ reactions: (a) NUSC, (b) USC, (c) USKC and (d) reactions with 0.1 g (1.3 wt.%) of $CaCO_3$.

tic acid coated $CaCO_3$. The synthesis of a polymeric nanocomposite is of interest in various fields as mentioned in Section 1. The incorporation was carried out at two different proportions (1.3 and 4 wt.% with respect to MMA). The NUS, US and USK MMA–$CaCO_3$ reactions are referred to as NUSC, USC and USKC, respectively and the conversion results are shown in Fig. 6.

The trends in conversion for all the MMA–$CaCO_3$ systems are similar to the MMA only reactions and the optimum temperature conditions (with respect to highest final conversion) were also the same, viz., 50 °C for the NUSC and USKC reactions and 30 °C for the USC reaction. The USCK reaction still showed a higher final conversion (86.1%) as compared to the NUSC reaction (76%). There-

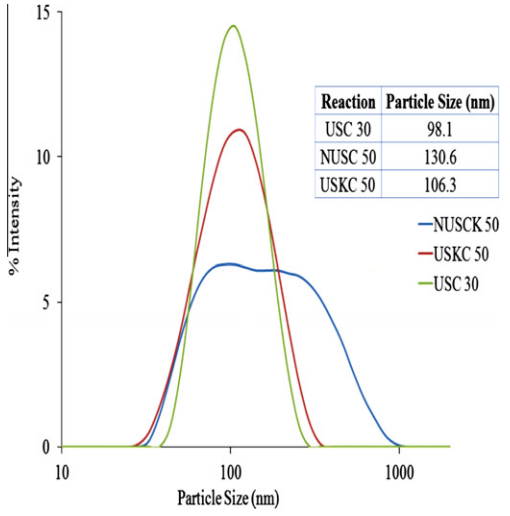

Fig. 7. Particle size distribution variation amongst the three syntheses with 4% incorporation of $CaCO_3$.

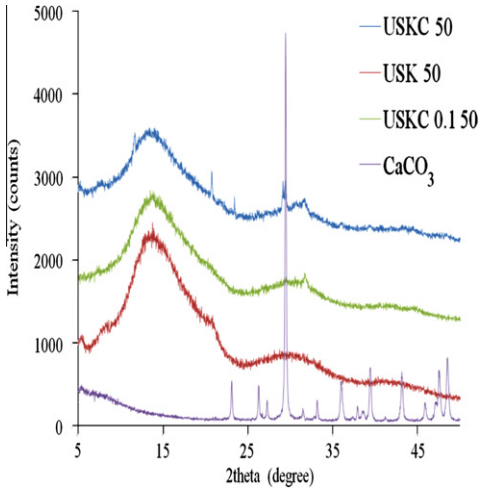

Fig. 8. XRD patterns of the samples prepared by US and KPS reactions for MMA only and MMA with varying $CaCO_3$ concentrations.

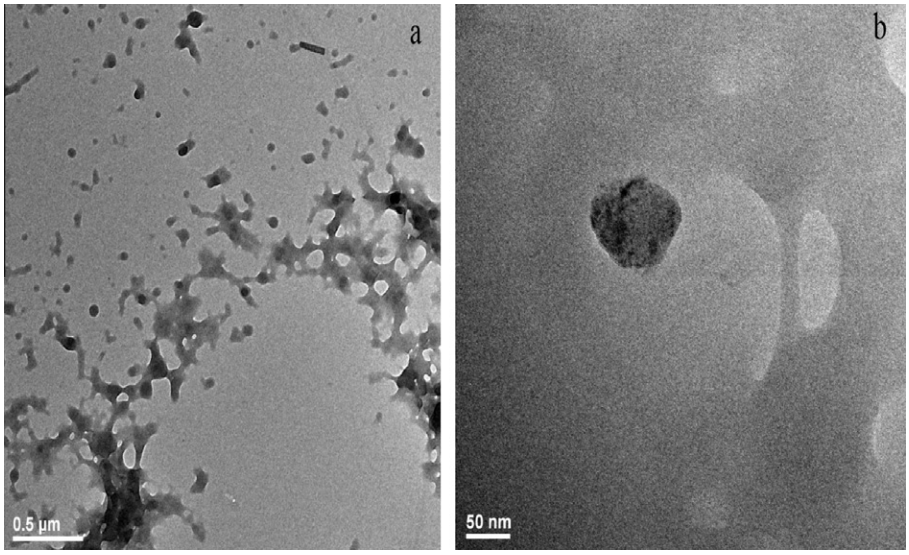

Fig. 9. (a) TEM image of USKC 0.1 50 at 500 nm. (b) TEM image of USKC 0.1 50 at 50 nm.

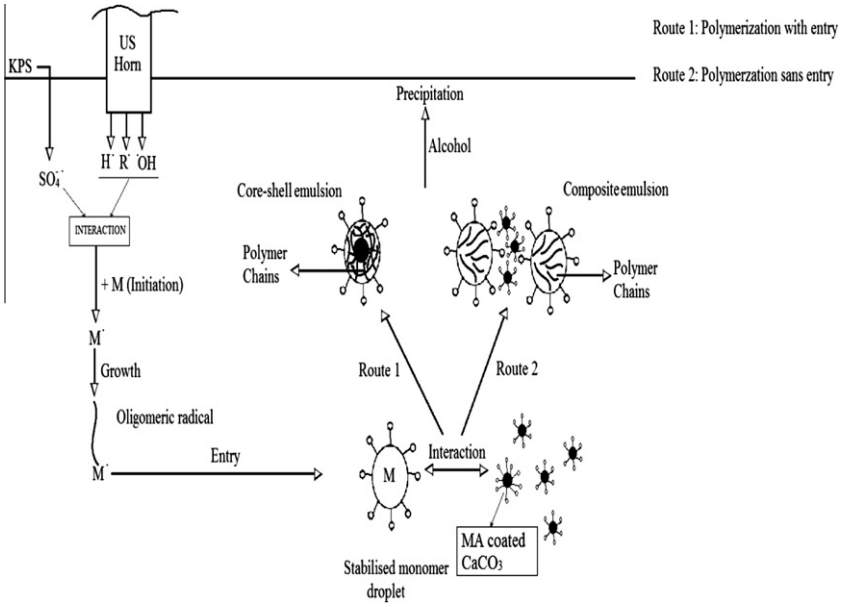

Fig. 10. Mechanism of USKC polymerization and particle formation.

fore, it can be concluded that the incorporation of $CaCO_3$ did not have any detrimental effect on the combination of the conventional and ultrasonic techniques. Wu et al. [36] have suggested that perhaps the incorporation of $CaCO_3$ could increase the rate of polymerization by accumulating on the monomer-water interface and providing more initiation sites. We noticed that although the final conversions did indeed slightly increase for the NUSC reactions as compared to the NUS reactions, no such effect was observed for the USC reactions under the reaction conditions used in this study.

To study a possible concentration effect of $CaCO_3$, the three syntheses showing the highest conversions (viz., NUSC 50, USC 30 and USKC 50) were carried out with a lower concentration of $CaCO_3$ (1.3 wt.% with respect to MMA). They were referred to as NUSC 0.1 50, USC 0.1 30 and USKC 0.1 50, respectively. The % conversion variation with time of these reactions is shown in Fig. 6d. Again the trends noticed were similar to those seen before, with the USKC 0.1 50 reaction showing the highest conversion (86.4%) amongst the three, continuing the trend that the combined use of US and KPS improves the final conversion. The USC reaction (USC 0.1 30) showed a trend similar to the USKC reaction but with a significantly lower final conversion.

The particle size distribution also follows a trend similar to the MMA only system (Fig. 7). The US (USC and USKC) reactions show a narrow particle size distribution as compared to the NUSC reactions. The reasons for that have already been discussed in the previous section. The reason why the average size is also higher than that observed in Fig. 5a is due to the incorporation of $CaCO_3$.

The XRD pattern (Fig. 8) of the MMA and MMA with varying amounts of $CaCO_3$ samples show that $CaCO_3$ is incoporated in the PMMA matrix as evidenced from the additional peaks in the pattern corresponding to that of $CaCO_3$ (crystallite size of 48 nm computed by using the Debye–Scherrer formula [37]). The presence of

the $CaCO_3$ peaks are more apparent in the 4% sample than in the 1.3% sample suggesting that the extent of coverage of the $CaCO_3$ particles by PMMA could be more extensive in the 1.3% sample.

Further analysis of the samples was carried out using TEM. For the PMMA–$CaCO_3$ specimen (USKC 0.1 50), two distinct phases corresponding to the PMMA and the $CaCO_3$ can be clearly observed (Fig. 9a). The spots on the micrograph indicate the formation of core–shell like structures (magnified in Fig. 9b) while there were also regions where a composite like structure (the darker $CaCO_3$ particles surrounded by the lighter PMMA particles) was observed.

On the basis of the results observed, a mechanism for the USKC reaction has been proposed as below (Fig. 10).

The mechanism initially is similar to the MMA only mechanism (Fig. 4), i.e., the formation of three sets of radicals as explained before, their subsequent interaction, reaction and neutralization, after which the remaining radicals initiate the polymerization and proceeds as described by Chern [26]. Either a composite particle or a core–shell particle is formed depending on whether the MA coated $CaCO_3$ particle enters the stabilized monomer droplet or just remains in its vicinity. If there is entry in addition to polymerization, a core–shell type structure resulted and if not, a composite structure was generated.

4. Conclusions

It has been observed that the combined use of ultrasound and potassium persulfate for the emulsion polymerization of MMA and MMA–$CaCO_3$ systems helps improve the overall conversion. While slower rates were observed for the combined system compared to NUS, narrow particle size distributions and smaller average particle sizes were obtained irrespective of the presence or absence of $CaCO_3$. On the basis of the observed results, a dual-pathway mechanism has been proposed for the formation of composite and core–shell PMMA–$CaCO_3$ nanoparticles.

Acknowledgements

K.P. would like to thank the University of Melbourne for providing the Melbourne International Fee Remission and Melbourne International Research Scholarships. M.A. acknowledges the financial support from the Australian Research Council (ARC-DP).

References

[1] M. Ashokkumar, T. Mason, "Sonochemistry", Kirk-Othmer Encylcopedia of Chemical Technology, John Wiley & Sons, 2007, doi: 10.1002/0471238961.1915141519211912.a01.pub2, Article online posting date: October 19, 2007.
[2] H. Grénman, E. Murzina, M. Ronnholm, K. Eranen, J. Millola, M. Lahtinen, T. Salmi, D.Y. Murzin, Enhancement of solid dissolution by ultrasound, Chem. Eng. Process. 46 (2007) 862–869.
[3] G.J. Price, New Methods of Polymer Synthesis, Blackie, Glasgow, UK, 1995.
[4] B.M. Teo, S.W. Prescott, M. Ashokkumar, F. Grieser, Ultrasound initiated miniemulsion polymerization of methacrylate monomers, Ultrason. Sonochem. 15 (2008) 89–94.
[5] C. Albano, G. Gonzalez, C. Parra, Sonochemical synthesis of polymethyl methacrylate to be used as biomaterial, Polym. Bull. 65 (2010) 893–903.
[6] G. Cooper, F. Grieser, S.R. Biggs, Butyl acrylate/vinyl acetate copolymer latex synthesis using ultrasound as an initiator, J. Colloid Interf. Sci. 184 (1996) 52–63.
[7] H. Xia, Q. Wang, Y. Liao, X. Xu, S.M. Baxter, R.V. Slone, S. Wu, G. Swift, D.G. Westmoreland, Polymerization rate and mechanism of ultrasonically initiated emulsion polymerization of *n*-butyl acrylate, Ultrason. Sonochem. 9 (2002) 151–158.
[8] S.K. Ooi, S. Biggs, Ultrasonic initiation of polystyrene latex synthesis, Ultrason. Sonochem. 7 (2000) 125–133.
[9] H.M. Cheung, K. Gaddam, Ultrasound-assisted emulsion polymerization of methyl methacrylate and styrene, J. Appl. Polym. Sci. 76 (2000) 101–104.
[10] Y. Kojima, S. Koda, H. Nomura, Effect of ultrasonic frequency on polymerization of styrene under sonication, Ultrason. Sonochem. 8 (2001) 75–79.
[11] B.A. Bhanvase, S.H. Sonawane, New approach for simultaneous enhancement of anticorrosive and mechanical properties of coatings: application of water repellent nano $CaCO_3$–PANI emulsion nanocomposite in alkyd resin, Chem. Eng. J. 156 (2010) 177–183.
[12] B.A. Bhanvase, D.V. Pinjari, P.R. Gogate, S.H. Sonawane, A.B. Pandit, Process intensification of encapsulation of functionalized $CaCO_3$ nanoparticles using ultrasound assisted emulsion polymerization, Chem. Eng. Process. 50 (2011) 1160–1168.
[13] B.A. Bhanvase, D.V. Pinjari, P.R. Gogate, S.H. Sonawane, A.B. Pandit, Synthesis of exfoliated poly(styrene-co-methyl methacrylate)/montmorillonite nanocomposite using ultrasound assisted in situ emulsion copolymerization, Chem. Eng. J. 181 (2012) 770–778.
[14] S.R. Shirsath, A.P. Hage, M. Zhou, S.H. Sonawane, M. Ashokkumar, Ultrasound assisted preparation of nanoclay bentonite-FeCo nanocomposite hybrid hydrogel: a potential responsive sorbent for removal of organic pollutant from water, Desalination 281 (2011) 429–437.
[15] S.S. Barkade, J.B. Naik, S.H. Sonawane, Ultrasound assisted miniemulsion synthesis of polyaniline/Ag nanocomposite and its application for ethanol vapor sensing, Colloid. Surf. A: Physicochem. Eng. Aspect. 378 (2011) 94–98.
[16] H.S. Xia, C.H. Zhang, Q. Wang, Study on ultrasonic induced encapsulating emulsion polymerization in the presence of nanoparticles, J. Appl. Polym. Sci. 80 (2001) 1130–1139.
[17] A. Gedanken, Doping nanoparticles into polymers and ceramics using ultrasound radiation, Ultrason. Sonochem. 14 (2007) 418–430.
[18] M. Avella, M. Errico, E. Martuscelli, Novel PMMA/$CaCO_3$ nanocomposites abrasion resistant prepared by an in situ polymerization process, Nano Lett. 1 (2001) 213–217.
[19] X. Xie, Q. Liu, R. Li, X. Zhou, Q. Zhang, Z. Yu, Y. Mai, Rheological and mechanical properties of PVC/$CaCO_3$ nanocomposites prepared by in situ polymerization, Polymer 45 (2004) 6665–6673.
[20] W.S. Zimmt, The emulsion polymerization of methyl methacrylate, J. Appl. Polym. Sci. 1 (1959) 323–328.
[21] J.G. Brondnyan, J.A. Cala, T. Konen, E.L. Kelley, The mechanism of emulsion polymerization I: studies of the polymerization of methyl methacrylates and *n*-butyl methacrylate, J. Colloid Sci. 18 (1963) 73–90.
[22] N.V. Kozhenikov, M.D. Goldfein, Kinetics of emulsion polymerization of methyl methacrylate and its copolymerization with acryl or methacrylamide, Polym. Sci. 33 (1991) 2255–2261.
[23] H.C. Chou, J.O. Stoffer, Ultrasonically initiated free radical-catalyzed emulsion polymerization of methyl methacrylate (II): radical generation process studies and kinetic data interpretation, J. Appl. Polym. Sci. 72 (1999) 827–834.
[24] Y. Liao, Q. Wang, H. Xia, X. Xu, S.M. Baxter, R.V. Slone, S. Wu, G. Swift, D.G. Westmoreland, Ultrasonically initiated emulsion polymerization of methyl methacrylate, J. Polym. Sci., Part A: Polym. Chem. 39 (2001) 3356–3364.
[25] M. Bradley, F. Grieser, Emulsion polymerization synthesis of cationic polymer latex in an ultrasonic field, J. Colloid Interface Sci. 251 (2002) 78–84.
[26] C.S. Chern, Emulsion polymerization mechanisms and kinetics, Prog. Polym. Sci. 31 (2006) 443–486.
[27] M.A. Bahattab, Polystyrene latex preparation in presence of ultrasonic initiation, J. Appl. Polym. Sci. 121 (2011) 2535–2542.
[28] B.A. Bhanvase, D.V. Pinjari, S.H. Sonawane, A.B. Pandit, Analysis of semibatch emulsion polymerization: role of ultrasound and initiator, Ultrason. Sonochem. 19 (2012) 97–103.
[29] S.W. Prescott, M.J. Ballard, R.G. Gilbert, Average termination rate coefficients in emulsion polymerization: effect of compartmentalization on free-radical lifetimes, J. Polym. Sci., Part A: Polym. Chem. 43 (2005) 1076–1089.
[30] I.M. Kolthoff, I.K. Miller, The chemistry of persulfate: I. The kinetics and mechanism of the decomposition of the persulfate ion in aqueous medium, J. Am. Chem. Soc. 73 (1951) 3055–3059.
[31] M.J. Ballard, D.N. Napper, R.G. Gilbert, Kinetics of emulsion polymerization of methyl methacrylate, J. Polym. Sci.: Polym. Chem. Ed. 22 (1984) 3225–3253.
[32] J.K. Rasmussen, S.M. Heilmann, P.E. Toren, A.V. Pocius, T.A. Kotnour, Kinetics and mechanism of the interaction of potassium peroxydisulfate and 18-crown-6 in aqueous media, J. Am. Chem. Soc. 105 (1983) 6845–6849.
[33] A.B. Ross, P. Neta, Rate constants for reactions of inorganic radicals in aqueous solution, Nat. Stand. Ref. Data Ser., Nat. Bur. Stand. (US) 65 (1979) 20.
[34] P. Maruthamuthu, Absolute rate constants for the reactions of sulfate, phosphate and hydroxyl radicals with monomers, Macromol. Chem., Rapid. Commun. 1 (1980) 23–25.
[35] J. Criquet, N.K.V. Leitner, Degradation of acetic acid with sulfate radical generated by persulfate ions photolysis, Chemosphere 77 (2009) 194–200.
[36] W. Wu, T. He, J. Chen, X. Zhang, Y. Chen, Study on in situ preparation of nano-calcium carbonate/PMMA composite particles, Mater. Lett. 60 (2006) 2410–2415.
[37] K. Prasad, D.V. Pinjari, A.B. Pandit, S.T. Mhaske, Phase transformation of nanostructured titanium dioxide from anatase-to-rutile via combined ultrasound assisted sol–gel technique, Ultrason. Sonochem. 17 (2010) 409–415.